

## Furnace Performance Analysis Fired with Oil Using Atomizers

Kyuil Han

National Fisheries University of Pusan

(Received April 12, 1990)

壓縮 空氣 噴射式 버너를 사용한 오일 燃燒時의  
燃燒爐 性能分析에 관한 研究

韓 圭 一

釜山水產大學校

(1990년 4월 12일 접수)

여러가지 다른 形態의 노즐을 空氣 旋回式 버너와 空氣의 旋回가 없는 버너(CB-125 Burner)에 裝置하여 空氣 噴射式으로 오일을 噴射하여 燃燒爐에서 燃燒시켰다. 燃燒爐는 길이 5m에 약 1m<sup>3</sup>의 燃燒空間을 가졌으며 상부에는 열전대를 裝置하고 하부에는 물이 흐르는 관을 設置하여 熱效率를 計算할 수 있게 設計하였다. 燃燒爐 煙突部에는 CO<sub>2</sub>, CO, O<sub>2</sub> 가스 分析器를 使用하여 過剩空氣量과 高溫計로 排氣가스 溫度를 測定하도록 하였다.

모든 測定値는 燃燒曲線과 效率曲線에 의하여 얻어진 常數를 利用하여 計算한 燃燒爐 性能方程式에 의하여 評價하였다. 實驗値에 의해 計算한 벽면 熱損失量과 熱傳達 公式에 의해 算出한 熱損失量을 比較 分析하여 測定値의 正確度를 推定하고 過剩空氣의 效果도 檢討하였다. 그結果 本研究에서 使用된 두 종류의 버너와 여러 形態의 노즐이 오일 연소시 熱效率 面에서 큰 差異를 보이지 않고 있음을 알았다.

### Introduction

This study describes the behavior of a hot wall furnace fired with #1 oil atomized with compressed air with the focus on the effect of the excess air and the performance of two different burners and several nozzles. The furnace used in the experiments described in this study is a hot-wall furnace with thermal loading by water-cooled tubes on the furnace floor that typically extracts 1/3 to 2/5 of the heat released<sup>1)2)</sup>.

This furnace was preferred at this time to using a boiler because of the design of thermal loading that provides a profile of the thermal flux down the furnace; this has been found in

past experiments to be usefully sensitive to both burner design and fuel type. The furnace also includes provision for probing along the flame. The hot-wall design does lessen some of the flame stability sensitivity to operational conditions. On the other hand, it is more closely representative of industrial furnaces which are a large though generally neglected potential market; it may also be more accurately representative of the resultant thermal flux on the flame to be found in larger water-wall boilers where the flame can only see a relatively small fraction of the water wall.

The focus in these experiments is on the furnace performance of firing #1 oil with a

**Table 1.** Fuel Properties

Fuel oil(#1)	
Heating Value(gross)	37,450 $MJ/m^3$ (19750 $Btu/lb$ )
Density at 15°C	0.8142
Sulfur	0.01%
Flash Point	63°C
Viscosity at 40°C	1.6cSt

comparison between the swirl burner and CB-125 burner using several different nozzles. The table 1 lists the relevant fuel oil data<sup>3)</sup>. The basis of the comparison is use of the firing and efficiency curves. These require measurements of the thermal input and output over a range of firing rates so that behavior under turn-down is an intrinsic part of the evaluation. Therefore, in this study the results of measurements of thermal efficiency are reported as a function of firing rate or output using #1 oil atomized by air.

## Experimental

### 1. Furnace

Essential construction of the furnace is a horizontal refractory box of square cross section of internal side 600mm and length 3m, generating 1.08m<sup>3</sup> of combustion space. The roof, walls and floor are insulation brick of 178mm thickness. The flat roof is set in as a jack arch. The whole furnace is cased in 3mm steel sheet, and the furnace stands on a steel skid framework with the combustion chamber center line 990mm above the floor.

The thermal load is provided by 30 square-section brass tubes(32×32mm) that are countersunk in the floor and water cooled; the tubes run across the width of the furnace and are equally spaced on 100mm centers. The water is supplied to each tube through constant flow orifices and through rotameters for continuous check. Each tube carries a thermistor at the outlet to determine the temperature rise across

each tube, with the inlet temperature monitored by two additional thermistors at each end of a common header supplying the array of the tubes.

The roof carries an array of 25 chromel-alumel thermocouples set in wells flush with the inside of the roof along the roof center line; the first 22 are 100mm apart and the last 3 are 200mm apart. An additional 5 TC's are set at different depths in the roof(0, 64, 114, 146, and 165mm)to monitor the temperature profile through the roof; these are set in approximately on the center line about 1m from the burner end.

### 2. Burner

The burner used for most of experiments is a variable swirl device<sup>4)</sup>; The burner is, in essence, a perforated can of length and diameter of 200mm with an air-blast atomizer gun up the center of the can. The air supply to the can is from a split annulus with air rotating in opposite directions in each half of the split. The annulus segments are fed from a common air line that divides into 2 pairs of lines with each pair feeding one of the two annular segments. Butterfly valves provide proportional control to each annulus segment, and swirl from full clockwise to full counterclockwise is obtained by altering the proportional division of air between the segments.

Initial experiments used a Cleaver-Brooks CB-125 burner which was found to be satisfactory for oil. It has effectively zero swirl and is designed to produce a long narrow flame in a range of boilers with flame tubes of substantially different length (L) and L/D ratios.

### 3. Ancillaries

Two air sources are used: compressed air for atomizing, and the main combustion air. The compressed air from the supply is metered through a 4" diameter Kurz mass flow meter (Model 505-11) based on hot wire(Pt)

anemometry with a range 15-150 *scfm* and with digital read-out in *scfm*. And the main combustion air is supplied from a Fuller rotary air compressor (type C-250) delivering up to 1 *lb/s* at 40 *psig*; it is metered through an 8" Kurz mass flow meter (Model 505-13) with a range 100 to 1000 *scfm* and with digital read-out in *scfm*. The signals of both mass flow meters are connected to a Datalogger.

No.1 oil is drawn from and standard 200 liter drum using a Sundstrand two-stage Model H pump at rates up to 0.02 *kg/s* and delivered to the furnace through a Model 12E Flow-Tron mass flow meter with remote digital read out in *lb/hr*.

Temperatures of the furnace roof, tube-bank

water, and exhaust gas are measured. The furnace roof temperature are measured with chromel-alumel TC's in closed end casings with the tips flush with the underside of the roof. Water temperature are measured at the inlet and outlet of the tubes using Yellw Springs Instrument Company thermistors (model YSI 701). The exhaust gas temperature is measured with a water-cooled suction pyrometer with a chromel-alumel element which is illustrated in Fig.1.

The exhaust gas is analysed on-line using two gas sampling probes at the furnace exit drawing samples for two independent sets of analyzers. One line analyses for O<sub>2</sub>, CO, and CO<sub>2</sub>(Fig.2).

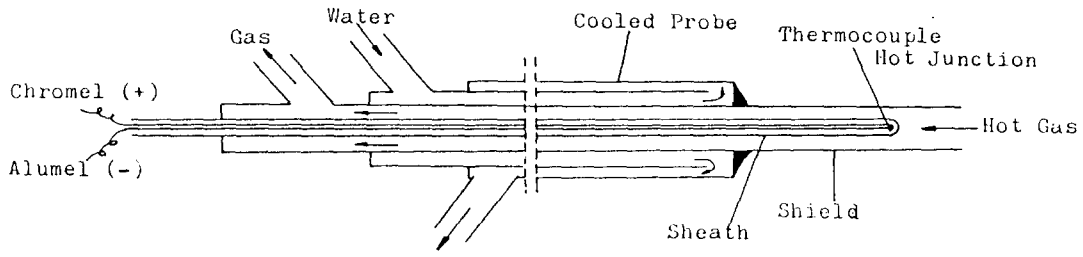


Fig. 1. Suction Pyrometer.

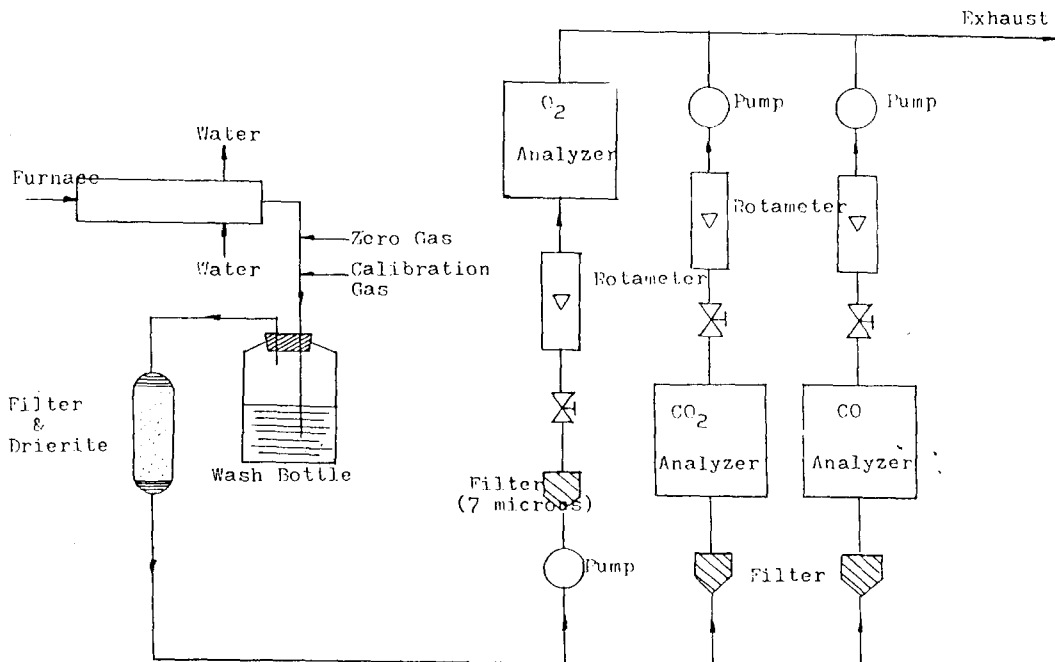


Fig. 2. CO<sub>2</sub>, CO, O<sub>2</sub> Gas Analysis Line.

#### 4. Ostwald Diagram

The consistency of the gas analyses is verified using the Ostwald Equations. These are also used to obtain the excess air percentage. The Ostwald equations provide the relations between the percentages of the four principal gases ( $O_2$ ,  $CO_2$ ,  $CO$ ,  $H_2$ ) and the excess air percentage ( $E\%$ ) on a dry basis. The relations between the percentages of the four gases can be given as

$$O_2\% = 21 - (0.79X_s + 0.21)CO_2\% - (0.79X_s - 0.19)CO\% + 0.19H_2\% \quad (1)$$

where  $O_2$ ,  $CO_2$ ,  $CO$  and  $H_2$  are the molar(volume) percentage concentrations on a dry basis, and  $X_s$  is the stoichiometric molar air/fuel ratio.

Because the percentage of  $H_2$  is difficult to get on a routine one-line basis, the approximation that  $H_2\% = 1/2 CO\%$  is used. Then, the relation between  $O_2\%$  and  $CO_2\%$ , with a  $CO\%$  correction can be given as

$$O_2\% = 21 - (0.79X_s + 0.21)CO_2\% - (0.79X_s - 0.28)CO\% \quad (2)$$

and, the relation between  $O_2$ ,  $CO_2$  and excess air percentage ( $E\%$ ) can be written

$$O_2\% [0.47 + (0.79 + E\%/100)X_s] = (21) [0.75 + X_s(E\%/100)] - CO_2\% [0.21 + (0.79 + 0.58 E\%/100)X_s] \quad (3)$$

where  $E\%$  is the excess air percentage.

As illustrated in Fig.3, Equations (2) and (3) show straight lines of negative slope when plotting  $O_2\%$  against  $CO_2\%$  at either constant  $CO\%$  or constant  $E\%$ ; and the equations represent two groups of parallel straight lines for different sets of values of  $CO\%$  or  $E\%$ . The values ( $CO$ ,  $CO_2$ ,  $O_2$ ) obtained from gas analysis must reasonably satisfy Eq. (2). If agreement is acceptable, Eq. (3) is used to determine the excess air percentage.

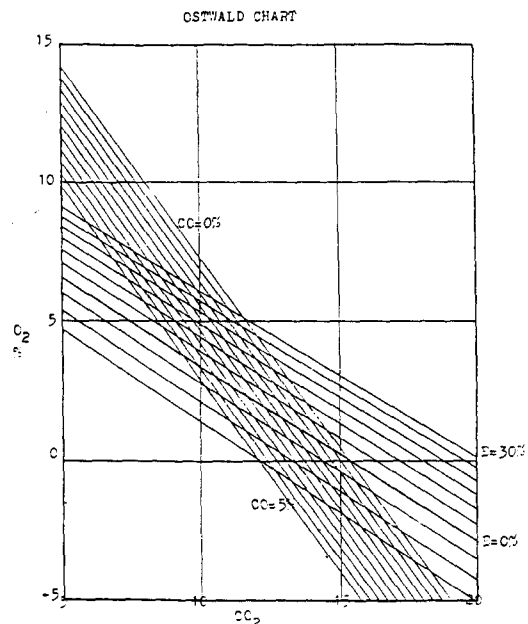


Fig. 3. Ostwald Diagram.

#### 5. Atomzer Nozzle

Table 2 includes several nozzle designed by us, CB-125 nozzle, two Monarch nozzles, and several Delavan nozzles. Acceptable atomization was always the principal problem. The CB-125 nozzle illustrated in Fig.4 was only used with the CB-125 burner; it performed satisfactorily with the

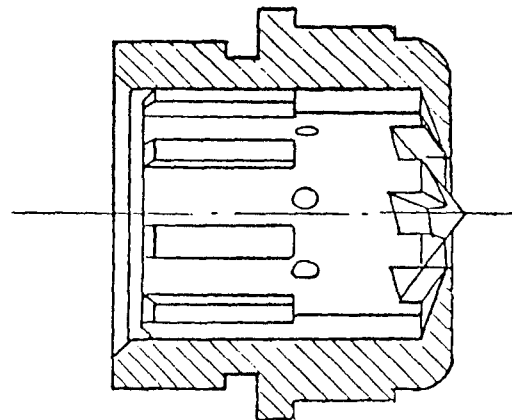


Fig. 4. CB-125 Nozzle.



## Furnace Performance Analysis Fired with Oil Using Atomizers

**Table 2. Summary of Nozzle Characteristics & Performance**

1. <u>Cleaver-Brooks-CB-125.</u>	Brass. Flame characteristics unknown.
2. <u>ME #1(in-house).</u>	Lowest flow resistance. Poorest atomization. Very narrow angle(30°C). No swirl. (Clearance too large).Flame improved with increased atomization pressure, but flame blew off with #1 oil.
3. <u>ME #2(in-house).</u>	Narrow angle(45°C). Atomizing air port 60° to oil port with offset to produce swirl. Still poor atomization and flame oscillated.
4. <u>ME #3(in-house).</u>	Same as ME #2 but with air port 90° to oil port. Poor atomization but no oscillations.
5. <u>Monarch B50.</u>	Swirled. Good to excellent atomization with good flames.
6. <u>Monarch A10</u>	Comple design. Very good oil flames.
	Clearances too small.
<u>Delavan "Swirl Air" Nozzles</u>	
7. <u>-#SL707-1(6 holes).</u>	Best nozzles of all. Swirled. Medium flow resistance. Very fine Atomization. Dazzling stable flame with oil.
8. <u>-#SL707-1 with SiC pintle(3 holes).</u>	Excellent flames above 50 psi atomization pressure. Still relatively poor turn down, but better than 6 hole atomizer.
9. <u>-#SL707-2</u>	Smaller pintle than for 707-1. Good flame but poorer atomization.
10. <u>-#SL707-3.</u>	Pintle too large. Poor atomization.
11. <u>Delavan "Airo" #301615-46</u>	Excellent for oil. Tip too small.

closed thermodynamic surface round the furnace is defined, a steady state energy balance across the system boundry yields

$$H_f = H_s + H_g + H_w \quad (4)$$

A special case of the general energy balance is the idle condition when the useful output( $H_s$ ) is zero and the energy supply rate is the minimum required to balance the wall losses when the boiler or furnace is otherwise at operating temperature. To denote the idle condition zero superscripts are used. So we have

$$H_f^o = H_w^o + H_g^o \quad (5)$$

Thring and Reber assumed the wall loss is substantially independent of output. The wall loss is now known to be a function of operating conditions, in general increasing with either firing rate or output, but the dependency is often not strong. Their argument was that wall losses are dominated by load temperature and this later, for engineering reasons, is maintained fairly constant. Thus

$$H_w \cong H_w^o \quad (6)$$

Consequently, the wall losses can be eliminated

by subtraction of Eq. (5) from Eq.(4).

The stack or exhaust gas enthalpy( $H_g$ ) is a variable that depends both on the firing rate and on the exhaust gas temperature or specific enthalpy. (This represents the point of departure from Thring and Reber's analysis). Thus we may write

$$H_g = F h_g = (F h_f) (h_g/h_f) = H_f (h_g/h_f) \quad (7)$$

where  $h_f$  is the heat of combustion or calorific value of the fuel; and  $h_g$  is the specific exhaust gas enthalpy per unit mass of fuel input (F), that from simple considerations of stoichiometry is proportional to the true specific exhaust gas enthalpy per unit mass of gas leaving. Using Equation (7) to transform  $H_g$  and  $H_g^o$ , then subtracting (5) from (4) and using (6) and (7) yields

$$H_f - H_f^o = H_f (h_g/h_f) - H_f^o (h_g^o/h_f) + H_s \quad (8)$$

Be adding  $H_f^o (h_g/h_f)$  to both sides, this equation can be rearranged. This yields

$$(H_f - H_f^o) (1 - h_g/h_f) = H_f^o (h_g - h_g^o) / h_f + H_s \quad (9)$$

To allow for the real possibility that the

exhaust gas temperature (and enthalpy) will rise with output,  $h_g$  can be expressed as a series expansion of  $H_s/H_s^m$ .  $H_s^m$  is a maximum output for the furnace as the firing rate goes to infinite. Finally we assume that we only need to consider the first two terms of the expansion. So. we can write

$$h_g = h_g^o [1 + \alpha (H_s + H_s^m)] \quad (10)$$

This equation can be rewritten :

$$h_g - h_g^o = (h_f - h_g^o) (H_s/H_s^m) \quad (11)$$

This formulation includes the boundary condition that  $h_g = h_g^o$  at zero output (the idle condition) ; and it also expresses the assumption that, at the maximum output ( $H_s = H_s^m$ ), the specific enthalpy of the fuel per unit mass of fuel will be  $h_f$ .

The specific enthalpy,  $h_g$ , in Equation (9) is eliminated by using Equation (11) and, if we rearrange the equation, the Firing Equation is obtained as

$$H_f = H_f^o + H_s / [\alpha^o (1 - H_s/H_s^m)] \quad (12)$$

where  $\alpha^o$  is a parameter grouping given by

$$\alpha^o = \alpha_o^o / (1 + \alpha_o^o H_f^o / H_s^m) \quad (13)$$

and  $\alpha_o^o$  is an upper limiting value of  $\alpha^o$  given by

$$\alpha_o^o = 1 - h_g^o / h_f \quad (14)$$

The firing curve described by the Firing Equation (12) is concave upwards and has a finite thermal input,  $H_f^o$ , at zero output.  $H_f$  goes to infinity as  $H_s$  goes to the maximum output,  $H_s^m$ .

### 2. Operational Efficiency

The variation of efficiency with output can then be obtained from the Firing Equation<sup>6)</sup>, thus

$$\eta = \frac{H_s}{H_f} = \frac{\alpha^o (1 - H_s/H_s^m) (H_s/H_s^m)}{\alpha^o (H_f^o/H_s^m) + [1 - \alpha^o (H_f^o/H_s^m)] (H_s/H_s^m)} \quad (15)$$

Characteristics of the curve obtained from Equation (15) is an inverted, asymmetric U-

shaped curve.

### 3. Intrinsic Efficiency

The intrinsic efficiency  $\alpha$  is in effect the basic efficiency with the wall losses calculated out. Since the quantity  $H_f^o$  represents the energy supply rate to balance the wall losses (assumed constant), the heat available for use is only  $(H_f - H_f^o)$ .  $H_f^o$  can be determined by extrapolation of the firing curve to zero output. The intrinsic efficiency,  $\alpha$ , can then be defined by

$$\alpha = H_s / (H_f - H_f^o) = \alpha^o (1 - H_s/H_s^m) \quad (16)$$

This equation shows that the intrinsic efficiency is the fraction of that available energy  $(H_f - H_f^o)$  that actually goes to useful output and, according to Eq.(16), declines linearly with output. From this line two other constants,  $\alpha^o$  and  $H_s^m$  can be obtained.  $\alpha^o$  is the maximum value of  $\alpha$ , and  $\alpha^o$  represents the maximum intrinsic efficiency when there is wall loss. To correct  $H_f^o$  to zero wall loss, Equation (13) may be used.

## Results

Furnace roof temperature profile using the (variable swirl) burner with oil at zero swirl is illustrated in Fig.7. With zero swirl, the peak temperature is seen to be about 2/3 of the way down the furnace or about 2m from the burner. It

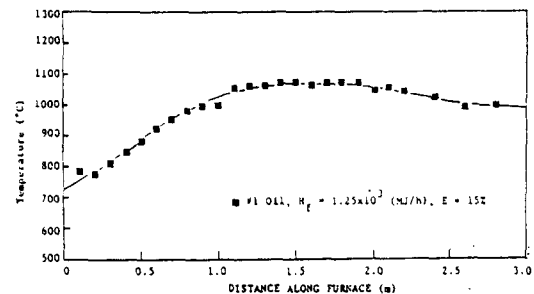
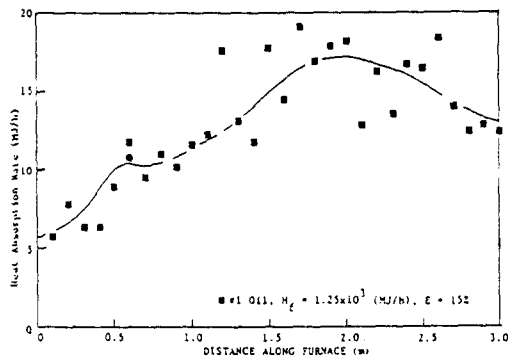


Fig. 7. Furnace Roof Temperature Profiles. Variation of Roof Temperature with Distance along Furnace for Oil.

## Furnace Performance Analysis Fired with Oil Using Atomizers

was evident that the outside recirculation gases that should have been carrying heat back to that root of the jet were being overcooled. The use of swirl eliminated this problem but at the same time required the use of wide angle nozzles (the Monarch and Delavan series).

Introduction of these three changes (swirl, increased spray angle, and gas atomization) essentially eliminated the small window of stability problem and permitted focus on atomization. The long flame at the burner end due to no swirl also modified the heat flux profile along the furnace length. This is illustrated in Fig. 8 which indicates the heat absorption rate in each floor tube for the same conditions as in Fig. 7. As can be expected from prior experience the flux profiles roughly mirror the roof temperature profiles.



**Fig. 8.** Heat Flux Profiles: Heat Absorbed in Each Floor Tube; Variation with Distance along Furnace for Oil.

Ostwald equations were used to check the consistency of the POC composition to determine the excess air, to cross-check the excess air values calculated from the input fuel and air rate data, and hence provide the POC mass flow rate. The gas analysis was used to determine the mass fraction of each constituent which, with the specific enthalpies from the gas temperature, yielded the POC enthalpy rate,  $H_g$ . The thermal output in the water tubes was calculated from the temperature rise and water flow rate;

summed for all the tubes. This gave the useful output,  $H_s$ .

Fig. 9 illustrates the thermal efficiency response against time. The graph shows the initial thermal efficiency starting at 8% as firing is started. With the furnace cold, the water tubes responded almost immediately to the firing so that a low thermal efficiency was measured due to the flame alone. As the walls and roof are heated up, the thermal efficiency increases in response to the wall contribution.

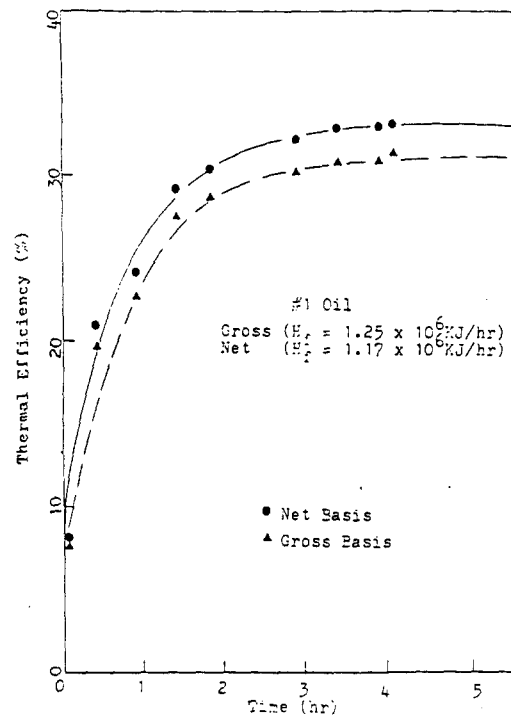


**Fig. 9.** Thermal Efficiency Variation against Time on Heat-Up by #1 Oil.

The wall loss is obtainable in principle by the following equation based on conduction through the wall and convection from the wall to ambient<sup>7)</sup>:

$$H_w = \int_A (T_w - T_o) / [(L/\lambda) + (1/h)] dA \quad (17)$$

where  $H_w$  is the wall loss;  $L$  is wall thickness;  $\lambda$  is the mean thermal conductivity of the



insulating fire brick ;  $T_w$  and  $T_o$  are the wall and ambient temperatures respectively ;  $h$  is the convection heat transfer coefficient from the outside wall to the ambient air ; and  $A$  is the furnace surface area. The resistance of the outside steel plate is regarded as negligible compared to the insulating fire bricks. This equation was used to make the rough estimate using the roof temperatures.

As can be seen, the oil data(Fig.10) show a roughly linear rise with output as expected ; in addition, the independent rough estimate of the wall loss, which is marked by an X on Fig.10(at 390 MJ/hr) was a little lower than the mean line. This suggests that the closure on the heat balance is reasonably good, possibly in the range 95 to 105%. Additional data points fired by the CB-125 burner are on the trend line of the swirl burner (with the CB-125 nozzle).

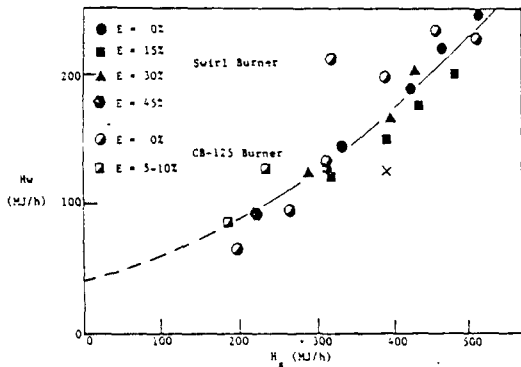


Fig. 10. Variation of Wall Loss ( $H_w$ ) with Output ( $H_s$ ) Firing Oil (2 burners) at 4 Levels of Excess Air (E%) with Trend Lines.

Fig.11 includes the data obtained with the CB-125 burner. The coefficients for drawing the curves were obtained from application of Eq.(16). Curve set shows the clear effects of excess air. As before, the data show clear trends with relatively little scatter and with good agreement with the data obtained using the CB-125 burner.

Fig. 12 illustrates the relation of the heat utilization factor against thermal output. The

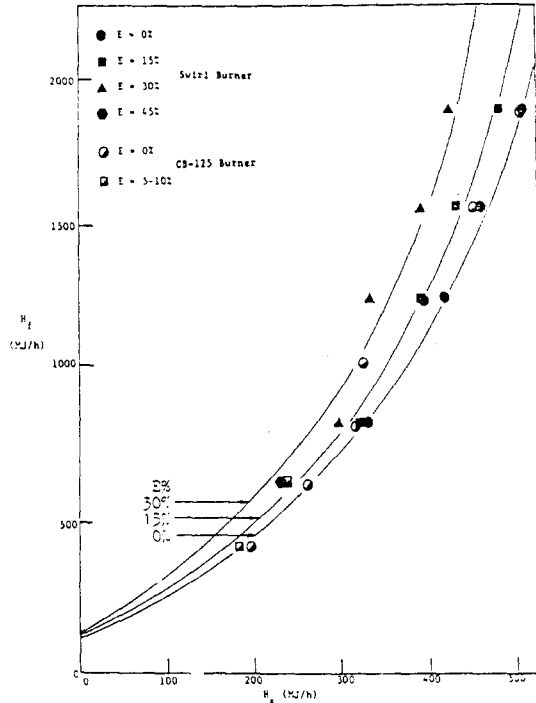
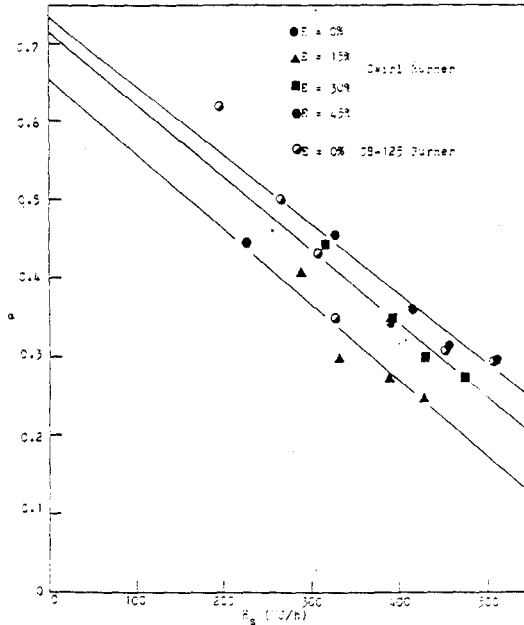


Fig. 11. Firing Curve for Oil (2 burners) : Variation of Thermal Input ( $H_t$ ) with Thermal Output in Water Tubes ( $H_s$ ) at 4 Levels of Excess Air (E%). (Lines are back-calculated).

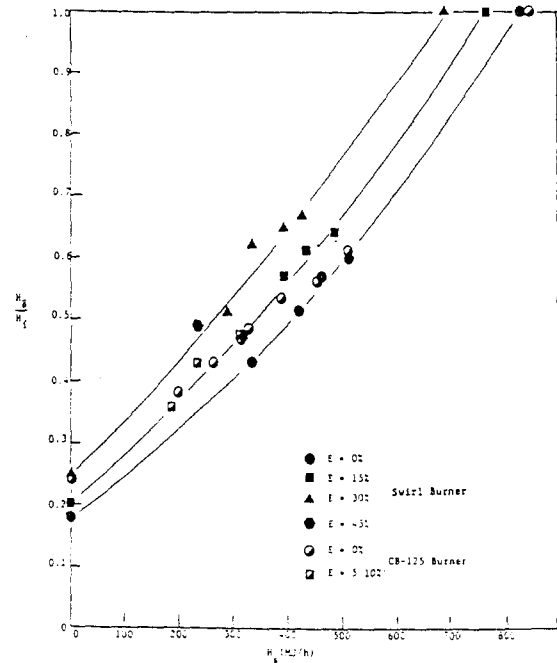
lines are described by Equation (16). On the assumption that Eq.(16) correctly describes the variation of  $\alpha$  with  $H_s$ , the best straight line through the experimental points yields the other two constants,  $\alpha^o$  and  $H_s^m$ , by extrapolation.

Fig. 13 illustrates the variation of thermal efficiency with output ; the curves are drawn using the relation (Eq. (15)) with  $H_t$  calculated from Eq. (12) using the coefficients. The specific enthalpy of the POC loss is a factor that is particularly sensitive to output. According to Eq. (11) it varies as a first approximation linearly with output. Fig. 14 shows the variation expressed as the specific ratio : heat units in the POC exhaust per heat unit entering( $H_g/H_f$ ). Data points obtained with the CB-125 burner are very close to the trend line of the swirl burner (with the CB-125 nozzle). The results are not exactly in accordance with Eq. (11) ; Fig. 14 shows that

## Furnace Performance Analysis Fired with Oil Using Atomizers



**Fig. 12.** Heat Utilization Factor Lines for Oil (2 burners): Variation of Heat Utilization Factor with Thermal Output ( $H_s$ ).



**Fig. 14.** Oil Firing (2 burners): Variation of POC Specific enthalpy ( $H_g/H_t$ ) with Thermal Output ( $H_s$ ), with Thend Lines.

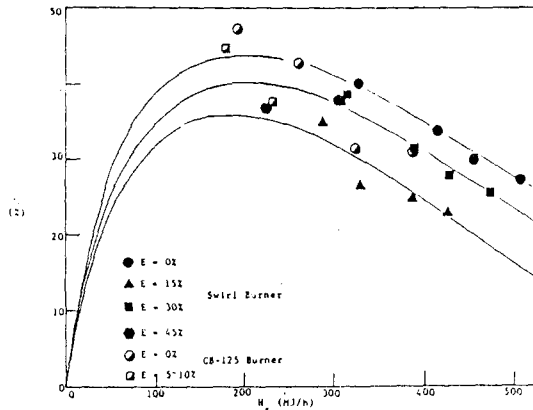


**Fig. 13.** Efficiency Curves for Oil (2 burners): Variation of Thermal Efficiency with Thermal Output ( $H_s$ ). (Lines are back-calculated).

the line in these experiments are slightly curved but the curvature is only about second order for the most part so that a straight line is a fair first approximation.

By a simple extension of the analysis a relation between the maximum output and excess air can be obtained. Writing

$$h_f = [1 + G_s(1 + E\%/100)] C_p (T_{ad,E} - T_s) \quad (18)$$

$$\text{and } h_f = (1 + G_s) C_p (T_{ad,o} - T_s) \quad (19)$$

where  $h_f$  is the heat of combustion or calorific value of the fuel;  $G_s$  is the stoichiometric air/fuel ratio;  $C_p$  is the mean specific heat of the exhaust gas;  $T_{ad,E}$  and  $T_{ad,o}$  are the adiabatic flame temperatures at excess air  $E\%$  and at zero excess air; and  $T_s$  is the load temperature.

If we equate Eqs. ((18) and (19) and rearrange, we obtain

$$\frac{T_{ad,E} - T_s}{[1 + G_s(1 + E\%/100)]} = \frac{(1 + G_s)(T_{ad,o} - T_s)}{[1 + G_s(1 + E\%/100)]} \quad (20)$$

In this furnace  $T_s$  is negligible compared to  $T_{ad}$ . Thus, we may approximate

$$T_{ad,E} = T_{ad,o}/F(E) \quad (21)$$

where  $F(E)$  is an excess air multiplier, given by

$$F(E) = [1 + G_s(1 + E\%/100)] / (1 + G_s) \quad (22)$$

To obtain the relation between maximum output and excess air, we consider the expressions

for the exhaust gas temperature ( $T_g$ ) and specific enthalpy ( $h_g$ ) at zero and  $E\%$  excess air ; thus

$$h_{g,E} = [1 + G_s(1 + E\%/100)] C_p (T_{g,E} - T_s) \quad (23)$$

$$\text{and } h_{g,o} = (1 + G_s) C_p (T_{g,o} - T_s) \quad (24)$$

Where  $h_{g,E}$  and  $h_{g,o}$  are the specific exhaust gas enthalpies at excess air  $E\%$  and at zero excess air ;  $T_{g,E}$  and  $T_{g,o}$  are the exhaust gas temperatures at excess air  $E\%$  and at zero excess air. If we assume that  $T_{g,E}$  and  $T_{g,o}$  must be the same if the excess air is changed, then using the same argument as before, we get

$$h_{g,E} = F(E) h_{g,o} \quad (25)$$

Likewise, at the idle condition

$$h_{g,E}^o = F(E) h_{g,o}^o \quad (26)$$

Using Eqs. (25), (26) and substituting Eqs. (11), (14), then finally we obtain

$$\begin{aligned} H_{s,E}^m / H_{s,o}^m &= \alpha_{o,E}^o / [\alpha_{o,o}^o F(E)] \\ &= 1/F(E) = \phi \end{aligned} \quad (27)$$

Values of  $H_{s,E}^m$  are plotted in Fig.15 which shows good agreement with Eq.(27). As the Figure shows,  $H_s^m$  is rising linearly as  $\phi$  increases.

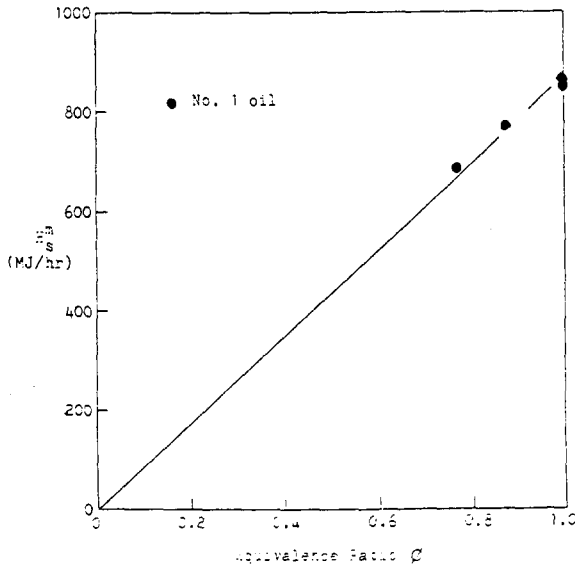


Fig. 15. Variation of Maximum Thermal Output  $H_s^m$  with Equivalence Ratio.

## Discussion and Conclusions

The system is a complex balance of heat exchange fluxes in the furnace. The primary source of heat is the flame, of course, but the heat received by the load (the water tubes) is provided by the following sources : direct radiation from the flame ; convection from the flame (generally less than 5% of the total received) ; direct radiation from the walls (with a fraction absorbed during transmission through the flame) ; radiation from the flame that was wall-directed but was absorbed by intervening gas and re-radiated to the load ; and wall-to-wall radiation that was absorbed by the gas and re-radiated to the load<sup>8</sup>). In a small furnace as much as 2/3 of the heat is derived from the roof and walls, with only 1/3 supplied directly from the flame. This proportioning is sensitive to the optical width and length of the furnace.

Flame emissivity plays a double role in this : if emissivity increases, the direct contribution from the flame increases (other things such as flame temperature being equal) but there will be an increase in the fraction of wall-to-load radiation that is absorbed by the flame. If the two factors of increased flame contribution and reduced wall contribution exactly balanced, there would be no change in thermal efficiency in a hot wall furnace as the flame emissivity changed. In general, the two factors do not balance but the offset is often sufficient in a hot wall furnace to make flame emissivity only a second order factor in controlling thermal efficiency.

Although a total check on measurement accuracy by determining the energy closure on the furnace was not possible because wall losses were not independently measured, nevertheless, the comparison of the wall losses obtained by the difference show expected trends and values, with losses in the range expected (5 to 15% of input).

The overall thermal efficiency would not necessarily change significantly since this is as much a matter of size of heat exchange surfaces

following the flame tube in a shell boiler, or following radiant combustion chamber of a water wall boiler. What would happen would be a change in the distribution to the heat absorbed in the combustion chamber and in the heat exchange passes. By definition, the heat exchange surfaces are "overdesigned" at reduced load so that the efficiency rises as load is reduced when the design point is at the output level that is greater than the optimum efficiency.

And the thermal efficiency did not show a big differences in this study of oil combustion using two kinds of burner (swirl burner, CB-125 burner) with different nozzles.

### References

- 1) Enomoto, H. (1971): An investigation of heat transfer in a continuous model furnace: a comparison of theory and experiment. Ph. D. Thesis, Pennsylvania State University.
- 2) Koval, A.A., S. Slupek, A. Kokkinos, A. Shaler, N.M. Miskovesky, and R.H. Essenhigh (1976): Smoke point and heat transfer characteristics of oil/water/air emulsions in a hot wall furnace. Spring Meeting, Central States Section of the Combustion Institute.
- 3) Spiers, H.M. (1937): Technical data on fuel. 4th edition, Brit. Nat. Comm. World Power Conf. London.
- 4) Faulkner, E.A. (1981): Guide to efficient burner operation: gas, oil and dual fuel. The Fairmont Press, Inc.
- 5) Essenhigh, R.H., A.C. Thekdi, G. Malhouitre and Y. Tasi (1974): Furnace analysis: a comparative study, Ch. 13 in Combustion technology: some modern developments. Academic Press.
- 6) Thring, M.W. and J.W. Reber (1945): The effect of output on the thermal efficiency of heating appliances. Journal of the Institute of Fuel 18, 12.
- 7) Holman, J.P. (1981): Heat transfer. 4th edition, MacGraw-Hill, New York.
- 8) Thring, M.W. (1952): The science of flame and furnaces. John Wiley and Sons, Inc., New York.